Electronic Supplementary Material (ESI) for Dalton Transactions.

Supporting Information for

Dehydrogenation of Hydrocarbons with Metal-Carbon Multiple Bonds and Trapping of a Titanium(II) Intermediate.

Anne K. Hickey, Marco G. Crestani, Alison R. Fout, Xinfeng Gao, Chun-Hsing Chen, and Daniel J. Mindiola†*

*mindiola@sas.upenn.edu

Department of Chemistry and Molecular Structure Center, Indiana University, Bloomington, Indiana 47405.

†*Present address: Department of Chemistry, University of Pennsylvania, 231 South 34th Street, Philadelphia, Pennsylvania 19104.*

General considerations.

Unless otherwise stated, all manipulations involving air- or moisture sensitive compounds were performed in double or single M. Braun Lab Master glove-boxes under purified nitrogen or argon atmospheres. All glassware used was either flame- or oven-dried overnight at 145 °C, and cooled down under dynamic vacuum before use. Celite, alumina, and 4 Å molecular sieves used for the purification of compounds and solvent drying were activated at 250 ºC for at least 24 h under high dynamic vacuum, before use.

Materials and methods.

Anhydrous hydrocarbon solvents (benzene, toluene, and *n*-pentane) were purchased from Aldrich in 20 L stainless-steel sure-sealed reservoirs and directly dispensed into the gloveboxes after passage through activated alumina and Q-5 drying agent columns installed in an M. Braun solvent purifier system (MB-SPS). Diethyl ether (Et_2O, Aldrich) was dried by dual passage through activated alumina columns. Tetrahydrofuran (THF, J.T. Baker) and 2,2,4-trimethylpentane (99+%; Alfa-Aesar) were dried and distilled from deep purple sodium/benzophenone ketyl solutions.[1] All bulk protio-solvents were kept over sodium and 4 Å molecular sieves. Deuterated solvents such as benzene-d_6 (C_6D_6, Cambridge Isotope Laboratories, CIL), toluene-d_8 (Aldrich) and cyclohexane-d_{12} (C_6D_{12}; CIL) were degassed by three consecutive freeze-pump-thaw (FTP) cycles in a Schlenk line and placed over sodium and molecular sieves for at least 12 h prior to use. Heptane (99 %) and cyclohexane (99.5 %) were purchased anhydrous from Aldrich and used without further purification. $[(PNP)Ti{=}CH^tBu(OTf)]$ (PNP = $N[2\text{-}P(CHMe_2)_2\text{-}4\text{-methylphenyl}]_2^-$, OTf = $[OSO_2CF_3]^-$) and $[(PNP)Ti{=}CH^tBu(CH_2{}^tBu)]$ were prepared according to the reported procedures by our group.[2] $LiCH_2{}^tBu$ was prepared in bulk amount from lithium (99 %, 0.5% w/w sodium; Aldrich).[3] All other chemicals, chromatographic materials and filter aids were purchased in high purity grade and used without further purification.

Characterization.

Unless otherwise stated, NMR spectroscopic characterization of all air and moisture sensitive compounds was done in solution using sealed J-Young NMR tubes, under argon. All 1D (^{1}H, *selectively* and *fully decoupled* ^{1}H{^{31}P}, ^{31}P{^{1}H}, ^{13}C{^{1}H}, DEPT-135) and 2D (dqfCOSY, C-H *coupled* and *decoupled* multiplicity-edited gHSQC) NMR spectra of isolated products were recorded from C_6D_6 solutions, using Varian 500, 400 or 300 MHz NMR spectrometers operating at 25 °C. For 1D NMR spectra, the standard notation A{B} indicates one nuclei has been decoupled from another. For heteronuclear 2D experiments, the notation A-B is used to indicate the specific type of correlation; with A and B being the different nuclei of interest (^{1}H, ^{13}C, ^{31}P). Acronyms listed for 1D and 2D NMR experiments are: DEPT = *Distortionless Enhanced Polarization Transfer*, dqfCOSY = *double quantum filtered Correlation Spectroscopy*, gHSQC = *gradient Heteronuclear Single Quantum Correlation*, HMBC = *Heteronuclear Multiple Bond Coherence*. ^{1}H, ^{1}H{^{31}P}, and ^{13}C{^{1}H} chemical shifts are reported referenced to the internal residual proton or carbon resonances of C_6D_6 (δ = 7.160 ppm). ^{31}P{^{1}H} NMR chemical shifts are reported relative to external H_3PO_4 (δ 0.0 ppm). For 1D NMR listings, data is reported including: 1) the chemical shift, 2) the multiplicity of the peak (*s* = singlet, *d* = doublet, *dd* = doublet of doublets, *t* = triplet, *m* = multiplet), 3) the *J*-coupling constant values, 4) the integration value, and whenever possible 5) the chemical assignment. The listings include: ^{1}H, ^{1}H{^{31}P} when available, ^{13}C{^{1}H} and ^{31}P{^{1}H} NMR. For 2D NMR, $<\delta_1, \delta_2>$ coordinates extracted from the C-H decoupled multiplicity-edited gHSQC spectra (δ_1 = ^{1}H and δ_2 = ^{13}C{^{1}H}) are reported for the select, key connectivities around titanium centers, consisting of the neopentyl-CH_2 moiety and the cross-peaks for the bound olefins. The one-bond coupling constant, $^1J_{C\text{-}H}$, in these fragments is reported as measured from the respective C-H coupled multiplicity-edited gHSQC bidimensional spectra. GC/MS analyses of organics were performed by manual injection into an Agilent Technologies 6890N Network GC system equipped with MS detector. Free olefins resulting from vacuum transferred were transferred into separate J-Young NMR tubes and checked by ^{1}H NMR. The Teflon valves in the receiving tubes J-Young tubes were then capped with rubber septa, the valves opened and 10 µL of gas from the headspace removed for injection into the GC/MS using a gas-tight syringe (Hamilton). No accurate CHN microanalyses of the independently prepared compounds could be obtained, due to their extreme sensitivity. We therefore provide high-resolution 1D and 2D NMR spectra in lieu of these data as proofs of their purity. Electronic spectra were collected using a Perkin-Elmer Lambda 19 spectrophotometer using UVWinlab software.

Summary of kinetics experiments.

All kinetics measurements were performed using sealed J-Young NMR tubes. The experiments were performed a minimum of two times to ensure consistency of data. Flame-sealed capillaries charged with dilute C_6D_6 solutions of PMe_3 (Aldrich; $^{31}P\{^1H\}$ NMR (162 MHz): δ -61.9 ppm, *s*) were used as internal standards. The tubes were charged with neat solutions of [(PNP)Ti=CH^{t}Bu(CH$_2$^{t}Bu)] (0.010 g, 0.016 mmol) with 2,2'-bipyridiyl in an argon glovebox. The tubes were closed, taken out from the glovebox and immediately placed in a 400 MHz NMR spectrometer with the temperature of the probe calibrated to ~29 °C. The temperature calibration was done using neat ethylene glycol (100%) prior to each experiment. The reactions were then monitored by arrays of $^{31}P\{^1H\}$ NMR spectra (162 MHz; 64 transients, 1.8 s per transient) acquired at fixed intervals of 280 s, over a period of 12-14 h after which times, ~90 % conversion of [(PNP)Ti=CH^{t}Bu(CH$_2$^{t}Bu)] to the respective product or mixture of products ensued. Reaction rates (*k*) were determined monitoring the decay of [(PNP)Ti=CH^{t}Bu(CH$_2$^{t}Bu)] across the arrays, normalizing the integrated spectra relative to the internal reference. The resulting decay curves were then fit to first-order kinetics plots using the general equation, $\ln[C] = -kt + \ln[C]_0$, where [C] correspond to the concentration of [(PNP)Ti=CH^{t}Bu(CH$_2$^{t}Bu)] (Figures S58-S67).

Synthesis of 1

[(PNP)Ti^{III}(CH$_2$^{t}Bu)(bipy$^{\bullet-}$)] (**1**): To a vial was added 70.0 (0.11 mmol) mg of (PNP)Ti=C^{t}Bu(CH$_2$^{t}Bu) and 10 mL cyclohexane. After dissolution, 23.4 mg (0.15 mmol) of 2,2-bipyridyl was added to the vial. The reaction stirred for 24 h and was taken to dryness. Pentane was added to the oily blue product, which was filtered through Celite and taken to dryness. An oily, dark blue product was obtained (50.3 mg, 0.072 mmol, 65% yield). X-ray quality crystals were grown out of a saturated ether solution at -35 °C for 72 h. ^{1}H NMR (25 °C, 500 MHz, C_6D_6): δ 10.06 (d, J = 6 Hz, 1H, C_5H_4N), 7.93 (d, J = 6 Hz, 1H, C_5H_4N), 7.31 (dd, J_1= 7.5 Hz, J_2 = 4.5 Hz, 1H, C_5H_4N), 7.27 (d, 1H, C_6H_3), 7.19 (d, J= 4.5 Hz, 1H, C_6H_3), 6.98 (d, J = 8.5 Hz, 1H, C_6H_3), 6.80 (dd, J_1 = 7.7 Hz, J_2 = 4.3 Hz, 1H, C_5H_4N), 6.67 (d, J = 8.0 Hz, 1H, C_6H_3), 6.48 (d, J = 8.5 Hz, C_6H_3), 6.34 (d, J = 8.5 Hz, 1H, C_6H_3), 5.63 (t, J = 7 Hz, C_5H_4N, 1H), 5.40 (t, J = 6.8 Hz, C_5H_4N, 1H), 5.25 (s, 1H), 4.47 (s, 1H), 2.91 (sextet, 1H), 2.77 (quintet, 2H, C*H*Me$_2$), 2.68 (septet, 1H, C*H*Me$_2$), 2.21 (s, 3H, Ar-C*H$_3$*), 2.06 (s, 3H, Ar-C*H$_3$*), 1.85 (dd, 3H, CH*Me$_2$*), 1.62 (m, 3H, CH*Me$_2$*), 1.48 (dd, 3H, CH*Me$_2$*), 1.39 (m, 6H, CH*Me$_2$*), 1.25 (m, 6H, CH*Me$_2$*), 1.17 (dd, 3H, CH*Me$_2$*), 1.07 (s, 9H, ^{t}*Bu*), 0.75 (dd, 3H, CH*Me$_2$*), -1.15 (broad s, 2H). ^{13}C{^{1}H} NMR (25 °C, 125 MHz, C_6D_6): δ 159.1 (d, C_6H_3), 156.1 (d, C_6H_3), 148.7, 148.5, 137.9, 133.8 (C_6H_3), 133.0 (C_6H_3), 131.6 (C_6H_3), 131.5 (C_6H_3), 123.5 (C_6H_3), 122.9, 121.8, 120.7, 118.3 (C_6H_3), 116.9, 116.1, 38.8, 35.2, 34.8, 27.1 (Ar-*Me*), 25.7 (Ar-*Me*), 24.2, 23.0, 22.6, 21.7, 21.3, 21.0, 20.2, 19.9, 19.5 (d, CHMe$_2$), 18.9 (CHMe$_2$), 17.8, 14.6 (CHMe$_2$). ^{31}P{^{1}H} NMR (25 °C, 162 MHz, C_6D_6): 53.97 (d, $J_{P\text{-}P}$ = 48.2 Hz), 37.06 (d, $J_{P\text{-}P}$ = 47.0 Hz).

Selected NMR Spectra of 1

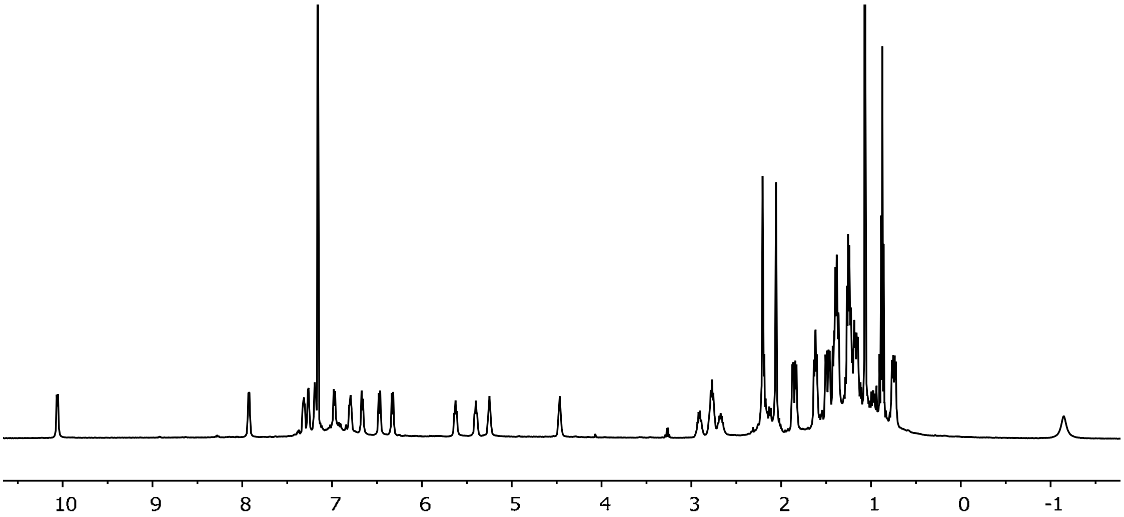

Figure S1: ^{1}H NMR spectrum of **1** in C_6D_6 (400 MHz, 25 °C).

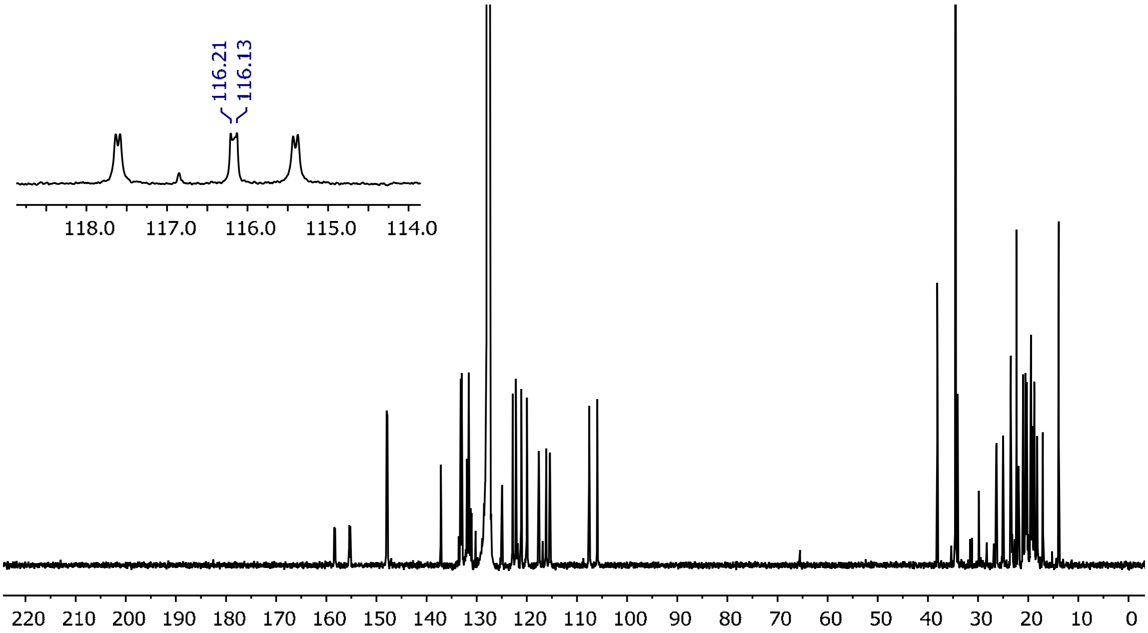

Figure S2: Expansion of the $^{13}C\{^{1}H\}$ NMR spectrum (125 MHz, 25 °C) of **1** in C_6D_6 at. No resonances downfield of 220 ppm were observed. Inset: the $^{13}C\{^{1}H\}$ resonance assigned to Ti-*C*H_2-^{t}Bu.

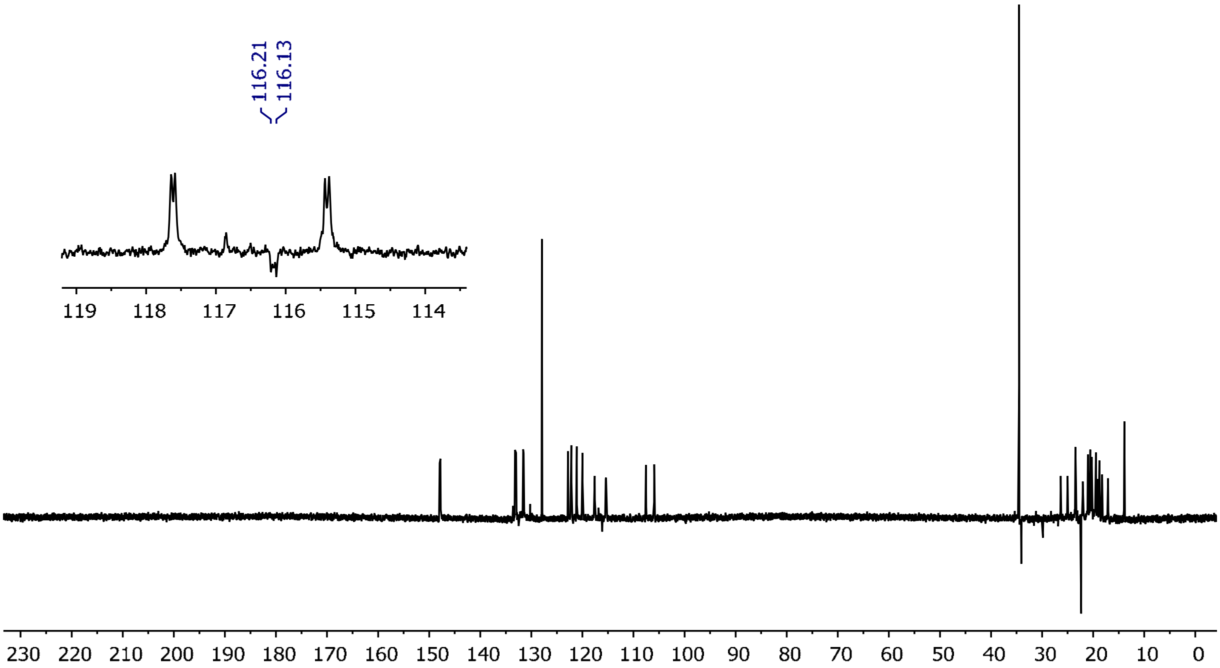

Figure S3: Expansion of the DEPT-135 NMR spectrum of **1** in C_6D_6. No resonances downfield of 220 ppm were observed. Inset: the resonance assigned to Ti-*C*H_2-^{t}Bu appears as a doublet at the same chemical shift as in the $^{13}C\{^1H\}$ NMR spectrum. The negative phase of this signal confirms the assignment of the hybridization of the Ti-*C*H_2-^{t}Bu moiety.

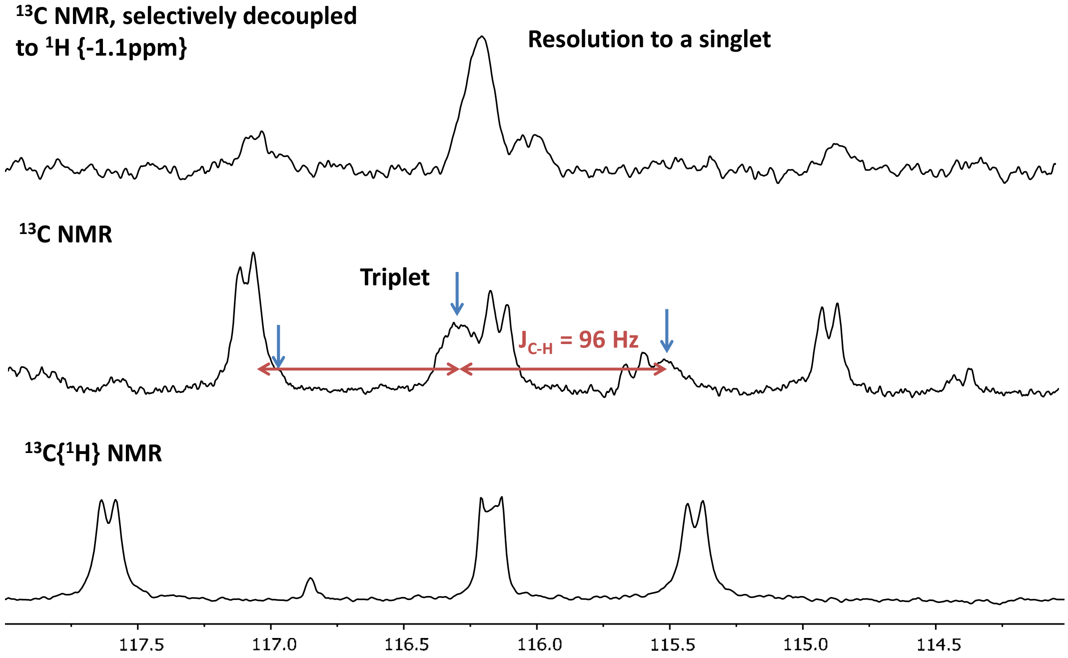

Figure S4: *Bottom*: ^{13}C{^{1}H} NMR spectrum in C_6D_6 (126 MHz, 25 °C); *Middle*: ^{13}C NMR spectrum (fully coupled, in C_6D_6, 126 MHz, 25 °C); *Top*: ^{13}C NMR spectrum (selectively decoupled to ^{1}H {-1.15 ppm}, C_6D_6, 126 MHz, 25 °C). The upfielded ^{1}H resonance at -1.15 ppm was assigned as two equivalent protons, evidenced by the triplet (blue arrows) observed upon full coupling (J_{C-H} = 96 Hz, red arrows) in the ^{13}C NMR spectrum. Upon full decoupling of this proton signal, the coupled carbon signal resolves from a triplet to a singlet, as expected for the multiplicity assignment of two equivalent H nuclei.

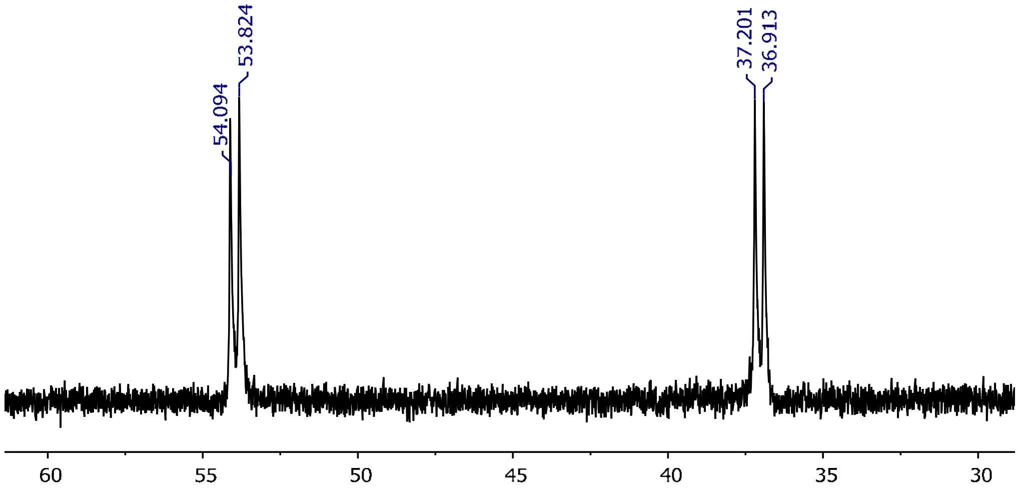

Figure S5: ^{31}P{^{1}H} NMR spectrum of **1** in C_6D_6 (162 MHz, 25 °C). ($^{2}J_{P-P}$ = 48 Hz).

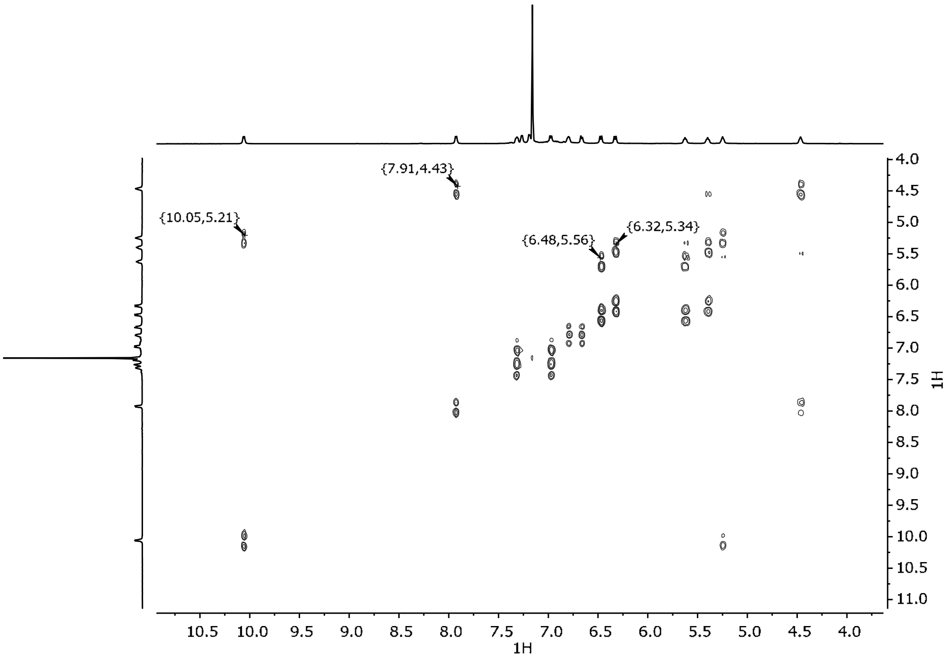

Figure S6: Expansion of the dqf-COSY spectrum of **1** in C_6D_6 at 25 °C.

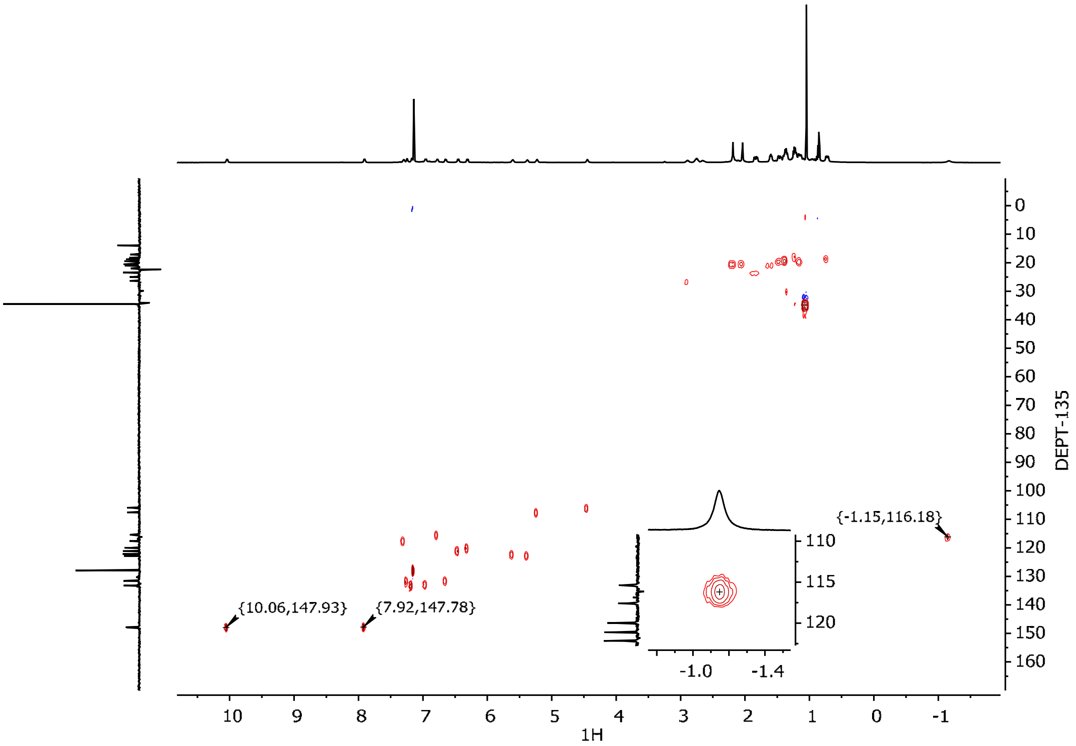

Figure S7: ^{1}H-^{13}C HSQC spectrum of **1** in C_6D_6 at 25 °C. The DEPT-135 spectrum is used to show a correlation (inset) of the proton at -1.147 ppm to the Ti-$\mathit{C}H_2$-^{t}Bu carbon. The unusual upfield shift of this proton could be attributed to an agnostic interaction with the Ti^{III} center.

Conversion of [(PNP)Ti=CH^{t}Bu(CH$_2$^{t}Bu)] to 1

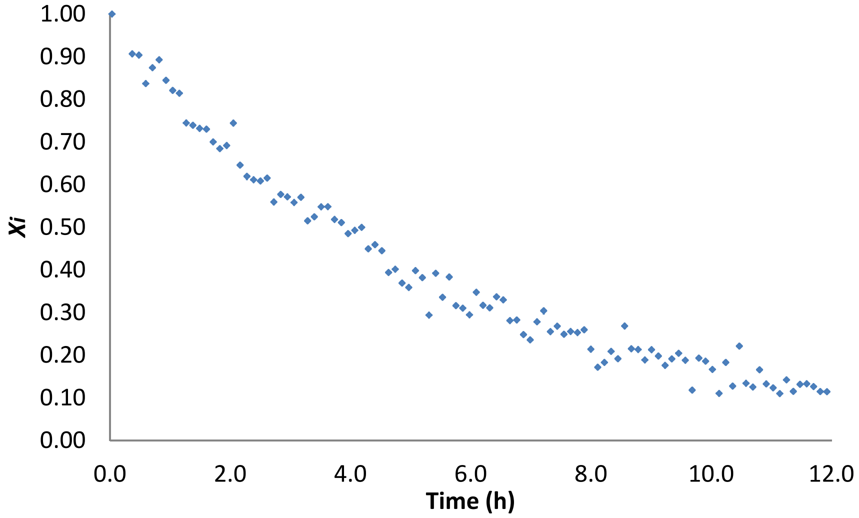

Figure S8: Decay of [(PNP)Ti=CH^{t}Bu(CH$_2$^{t}Bu)] in cyclohexane.

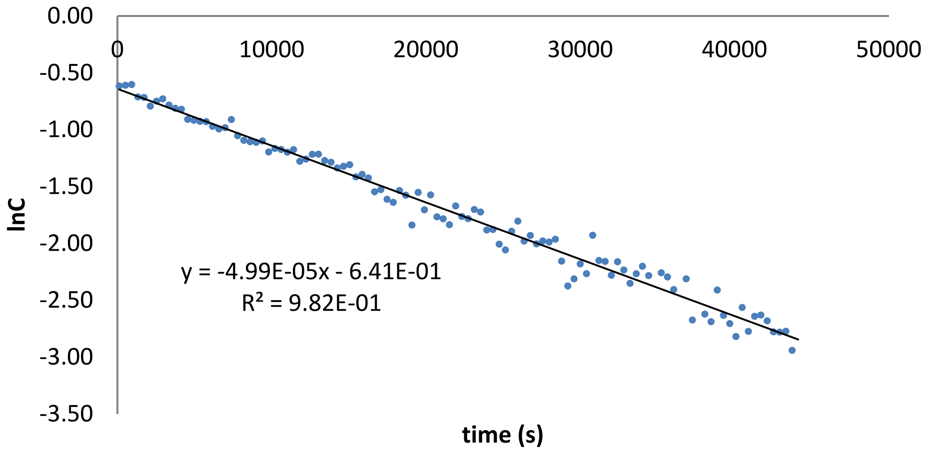

Figure S9: Logarithmic plot for decay of [(PNP)Ti=CH^{t}Bu(CH$_2$^{t}Bu)] in cyclohexane, adjusted for the equation: $\ln[\mathbf{C}] = -kt + \ln[\mathbf{C}]_0$. The half-life of [(PNP)Ti=CH^{t}Bu(CH$_2$^{t}Bu)] in solution is 3.8 h.

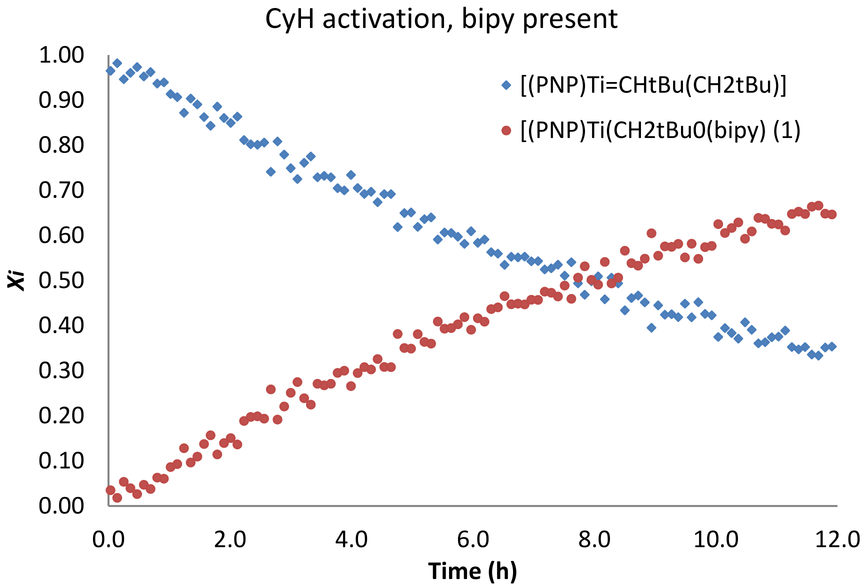

Figure S10: Consumption of [(PNP)Ti=CH^{t}Bu(CH$_2$^{t}Bu)] and formation of **1** in cyclohexane.

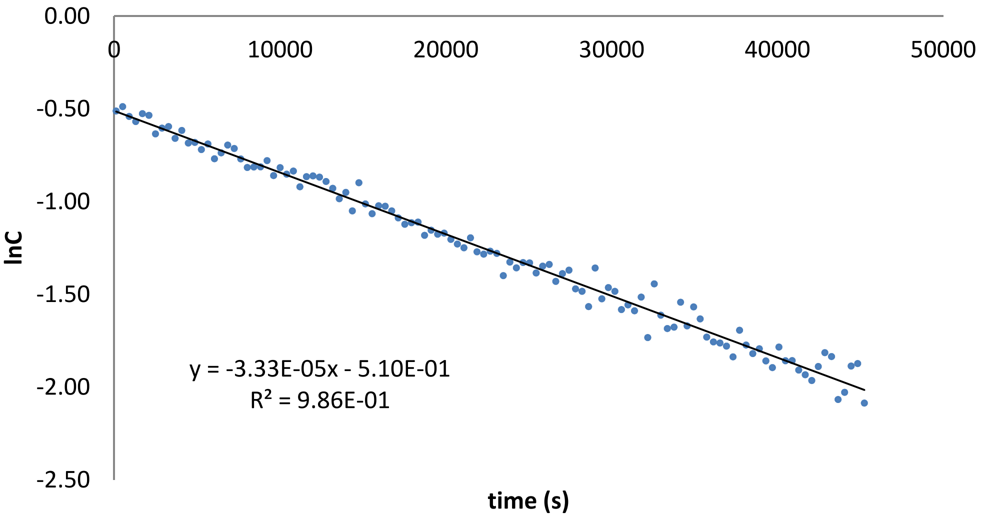

Figure S11: Logarithmic plot for decay of [(PNP)Ti=CH^{t}Bu(CH$_2$^{t}Bu)] in cyclohexane in the presence of bipy to form **1**, adjusted for the equation: ln[**C**] = -*kt* + ln[**C**]$_0$. The half-life of [(PNP)Ti=CH^{t}Bu(CH$_2$^{t}Bu)] is 5.8 h.

Mechanistic study: Changing the alkane solvent to heptane, C_7H_{16}

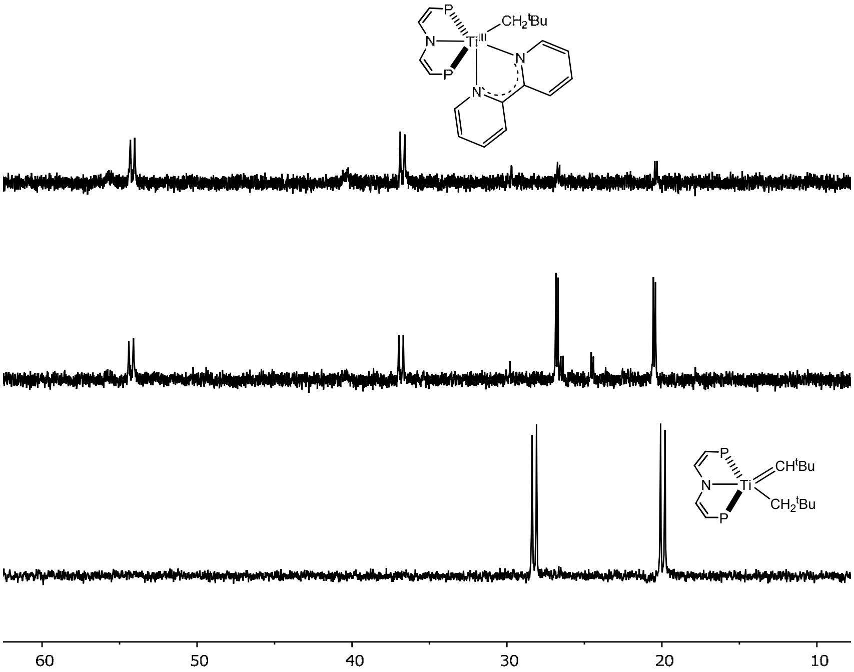

Figure S12: Running the reaction in heptane and monitoring by $^{31}P\{^1H\}$ NMR spectra (162 MHz, 25 °C) shows that **1** forms (54 and 36 ppm).

Mechanistic study: Changing the solvent to benzene, C_6H_6

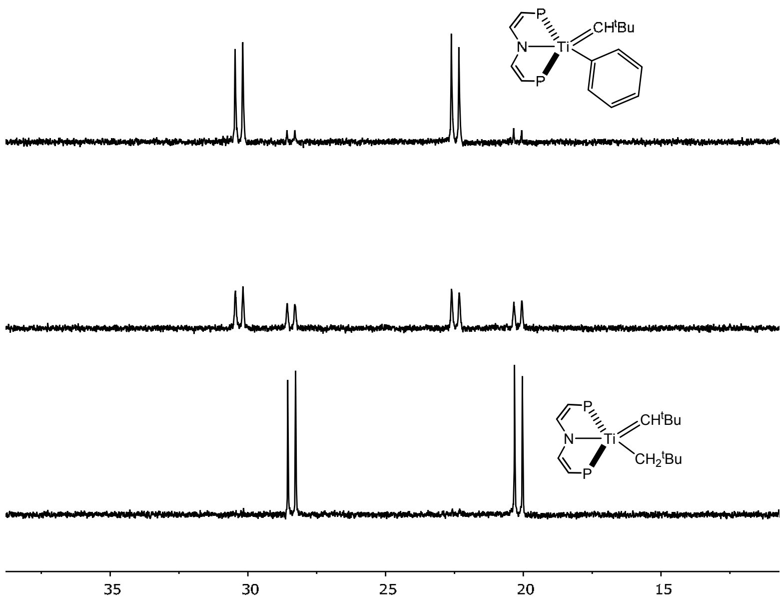

Figure S13: Changing the solvent to C_6H_6 only forms the known complex $[(PNP)Ti(CH_2{}^tBu)(C_6H_5)]$[8] , observed by $^{31}P\{^1H\}$ NMR spectra (162 MHz, 25 °C).

UV-Vis characterization of 1.

UV-Vis characterization was performed on diluted solutions prepared from a stock solution of 1.432 E-4 M of **1** in C_6H_6.

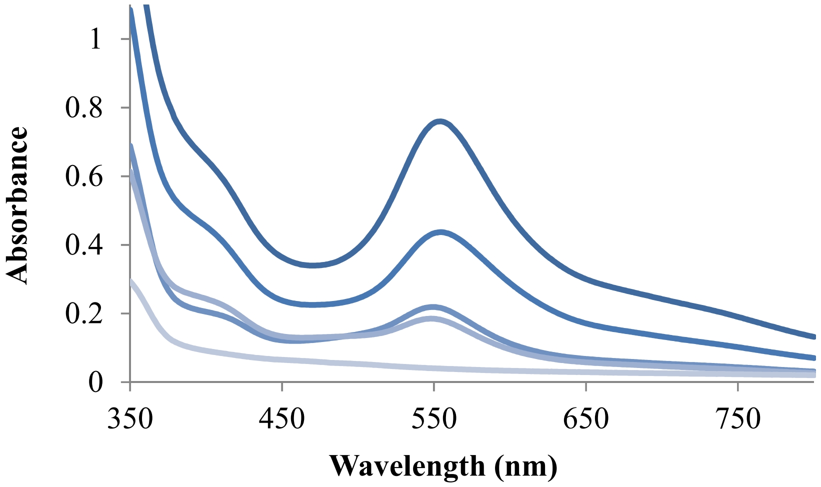

Figure S14: Absorbance versus wavelength for several solutions of **1** in C_6H_6. The broad signal at 554 nm (~18,000 cm^{-1}) indicate MLCT characteristic of π-radical anions.

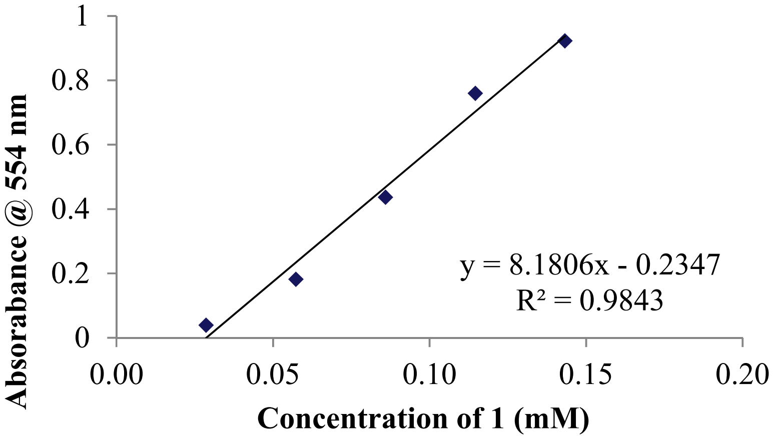

Figure S15: Absorption at 554 nm versus concentration of **1** in C_6H_6. The molar absorptivity ε for **1** was determined to be 8,181 $M^{-1}cm^{-1}$ at this wavelength. This order of magnitude is consistent with metal-ligand charge transfer.

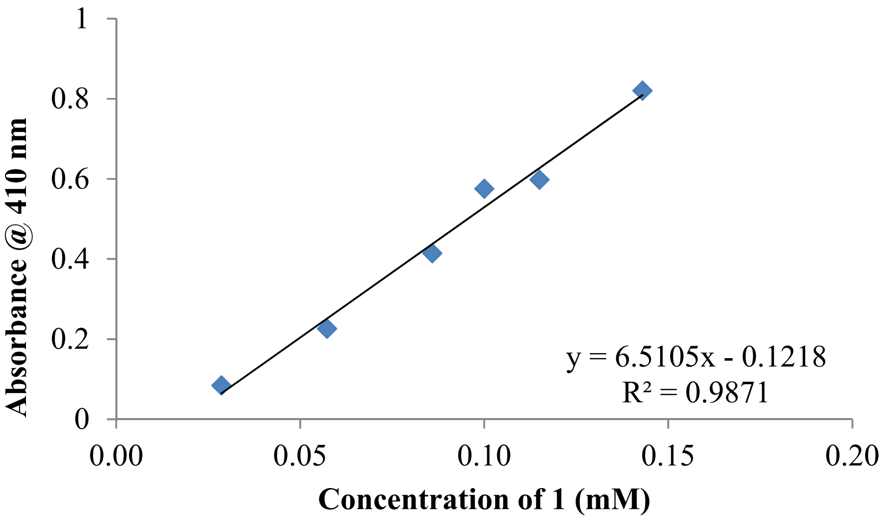

Figure S16: Absorption at 410 nm versus concentration of **1** in C_6H_6. The molar absorptivity ε for **1** was determined to be 6,5101 $M^{-1}cm^{-1}$ at this wavelength. The transition has been assigned as p→ p* within the bipy ligand.

Crystallographic Details for 1.

A purple crystal of **1** grown from a cold (-35 °C) diethyl ether solution was placed onto the tip of a 0.1 mm diameter glass capillary and mounted on a Bruker APEX II Kappa Duo diffractometer equipped with an APEX II detector at 150(2) K. The data collection was carried out using Mo Kα radiation (graphite monochromator) with a frame time of 40 seconds and a detector distance of 5.00 cm. A collection strategy was calculated and complete data to a resolution of 0.82 Å with a redundancy of 4 were collected. Six major sections of frames were collected with 0.50º ω and φscans. Data to a resolution of 0.82 Å were considered in the reduction. Final cell constants were calculated from the xyz centroids of 5129 strong reflections from the actual data collection after integration (SAINT).[4] The intensity data were corrected for absorption (SADABS).[5] Please refer to Table S1 for additional crystal and refinement information. The space group $P2_1/c$ was determined based on intensity statistics and systematic absences. The structure was solved using SIR-2004[6] and refined with SHELXL-97.[7] A direct-methods solution was calculated, which provided most non-hydrogen atoms from the E-map. Full-matrix least squares/difference Fourier cycles were performed, which located the remaining non-hydrogen atoms. All non-hydrogen atoms were refined with anisotropic displacement parameters. The hydrogen atoms were placed in ideal positions and refined as riding atoms with relative isotropic displacement parameters. The final full matrix least squares refinement converged to R1 = 0.0477 and wR2 = 0.1324 (F2, all data).

Table S1. Crystal data and structure refinement for 1

Empirical formula	C41 H59 N3 P2 Ti
Formula weight	1169.26
Crystal color, shape, size	Purple plate, 0.24 x 0.17 x 0.05 mm^3
Temperature	150(2) K
Wavelength	0.71073 Å
Crystal system, space group	Monoclinic, $P2_1/c$
Unit cell dimensions	a = 16.5848(5) Å α = 90°.
	b = 12.0621(3)Å β = 112.7370(10)°.
	c = 20.9865(6) Å γ = 90°.
Volume	3872.04(19) $Å^3$
Z	4
Density (calculated)	1.210 Mg/m3
Absorption coefficient	0.375 mm-1
F(000)	1504
Data collection	
Diffractometer	APEX II Kappa Duo, Bruker
Theta range for data collection	2.61 to 25.02°.
Index ranges	-19<=h<=19,
	-8<=k<=14,
	-24<=l<=21
Reflections collected	17573
Independent reflections	7720 [R(int) = 0. 1381]
Observed Reflections	6814
Completeness to theta = 25.02°	99.2 %
Solution and Refinement	
Absorption correction	Semi-empirical from equivalents
Max. and min. transmission	0.9635 and 0.9288
Solution	Direct methods
Refinement method	Full-matrix least-squares on F2
Weighting scheme	$w = [\sigma^2Fo^2+AP^2]^{-1}$, with $P = (Fo^2+ 2Fc^2)/3$, A

	= 0.0388
Data / restraints / parameters	7720 / 159 / 369
Goodness-of-fit on F^2	0.799
Final R indices [I>2sigma(I)]	$R_1 = 0.0516$, $wR_2 = 0.0942$
R indices (all data)	$R_1 = 0.1580$, $wR_2 = 0.1167$
Largest diff. peak and hole	0.410 and -0.275 e.Å^{-3}

Goodness-of-fit = $[\Sigma[w(Fo^2 - Fc^2)^2]/N_{observns} - N_{params})]^{1/2}$, all data.

$R1 = \Sigma(|Fo| - |Fc|) / \Sigma |Fo|$. $wR2 = [\Sigma[w(Fo^2 - Fc^2)^2] / \Sigma [w(Fo^2)^2]]^{1/2}$

XI. References.

1. R. J. Errington, Advanced practical inorganic and metalorganic chemistry, Blackie Academic & Professional, London, UK, 1st ed. (**1997**), pp. 92-107.
2. (a) B. C. Bailey, J. C. Huffman, and D. J. Mindiola, *J. Am. Chem. Soc.,* 2007, **129**, 5302–5303; (b) B. C. Bailey, J. C. Huffman, D. J. Mindiola, W. Weng, and O. V. Ozerov, *Organometallics,* 2005, **24**, 1390–1393.
3. (a) R. R. Schrock, and J. D. Fellmann, *J. Am. Chem. Soc.,* 1978, **100**, 3359–3370; (b) N. Ekizoglou, and N. Hadjichristidis, *J. Polym. Sci., Part A: Polym. Chem.,* 2001, **39**, 1198–1202.
4. SAINT, Bruker Analytical X-Ray Systems, Madison, WI, current version.
5. An empirical correction for absorption anisotropy. R. Blessing, *Acta Cryst.* 1995, **A51**, 33-38.
6. Sir2004, A Program for Automatic Solution and Refinement of Crystal Structures. M. C. Burla, R. Caliandro, M. Carnalli, B. Carrozzini, G. L. Cascarano, L. De Caro, C. Giacovazzo, G. Polidori, and R. Sagna. Vers. 1.0 (2004).
7. A short history of *SHELX*. G. M. Sheldrick, *Acta Cryst*., 2008, **A64**, 112-122.
8. B. C. Bailey, H. Fan, E. W. Baum, J. C. Huffman, M.-H. Baik, and D. J. Mindiola, *J. Am. Chem. Soc.*, 2005, **127**, 16016-16017.